

Immobilization of Bisphosphinoamine Linkers on Silica: Identification of Previously Unrecognized Byproducts via ³¹P CP/MAS and Suspension HR-MAS Studies

T. Posset, F. Rominger, and J. Blümel*

Organisch-Chemisches Institut, Universität Heidelberg, Im Neuenheimer Feld 270,
69120 Heidelberg, Germany

Received October 8, 2004. Revised Manuscript Received November 18, 2004

A new bisphosphinoamine linker with ethoxysilyl group has been synthesized and applied for anchoring nickel catalysts to alumina and silica. Side reactions occurred, and the reactions of various bisphosphinoamine ligands with silica were studied by ³¹P CP/MAS and suspension HR-MAS NMR. Besides the desired immobilization, two main side reactions have been found. The phosphine moieties of the linkers can be quaternized by ethyl groups from the ethoxysilyl functions. Furthermore, the bisphosphinoamine group can rearrange to the corresponding phosphinimine unit that is subsequently hydrolyzed, resulting in the amine and tetraphenyldiphosphine oxide. The latter is bound firmly to the silica surface.

Introduction

Binding molecules to oxidic surfaces in a clean and well-defined manner is of established importance in a variety of different areas, such as combinatorial chemistry,¹ solid-phase synthesis,² chromatography,³ and catalysis.⁴ In our endeavor to optimize catalysts⁵ we, and also countless other groups,⁶ have been active in the last field, improving the recyclability and lifetime of homogeneous rhodium and nickel catalysts by anchoring them on oxidic supports.^{7–9} For surface chemistry in general solid-state NMR spectroscopy¹⁰ proves

to be an indispensable and powerful analytical method. We recently optimized the cross-polarization (CP) process at higher magic angle spinning (MAS) frequencies¹¹ for our applications in order to improve the signal-to-noise ratio (S/N), and added stationary and high-resolution (HR) MAS suspension NMR spectroscopy¹² to our repertoire that allows us to study mobilities of surface species, as well as their reactivity with oxidic surfaces, and their structural nature.

Being thus equipped, we could optimize the immobilization procedure for metal complexes with bifunctional phosphines, such as the popular Ph₂P(CH₂)₃Si(OEt)₃ or chelating phosphines with ethoxysilane groups.^{7–9,13} We have studied the effect of the solvent on the immobilization process,¹⁴ and determined by ²⁹Si CP/MAS that only nonpolar solvents give optimal surface coverages.^{14b} The strongest bond is formed to silica and neutral alumina.^{12b} This is an important point, since weak, reversible binding leads to the well-known and feared leaching of catalysts, the detachment of the metal complex and/or the linker from the support.^{9,12b} Furthermore,

* Corresponding author. Telephone: (+49)6221-548470. Fax: (+49)6221-544904. E-mail: J.Bluelmel@urz.uni-heidelberg.de.

- (1) (a) *Handbook of Combinatorial Chemistry*; Nicolaou, K. C., Hanko, R., Hartwig, W., Eds.; Wiley-VCH: Weinheim, 2002; Vols. 1 and 2. (b) *Combinatorial Chemistry*; Wilson, S. R., Czarnik, A. W., Eds.; John Wiley & Sons: New York, 1997. (c) *Combinatorial Chemistry*; Bannworth, W., Felder, E., Eds.; Wiley-VCH: Weinheim, 2000. (d) Jung, G. *Combinatorial Chemistry*; Wiley-VCH: Weinheim, 1999.
- (2) (a) Seneci, P. *Solid-Phase Synthesis and Combinatorial Technologies*; John Wiley & Sons: New York, 2000. (b) Dörwald, Z. F. *Organic Synthesis on Solid Phase*; Wiley-VCH: Weinheim, 2000.
- (3) (a) Vansant, E. F.; VanDer Voort, P.; Vrancken, K. C. *Characterization and Chemical Modification of the Silica Surface*; Elsevier: Amsterdam, 1995. (b) Scott, R. P. W. *Silica Gel and Bonded Phases*; John Wiley and Sons: New York, 1993. (c) Subramanian, G. A. *Practical Approach to Chiral Separations by Liquid Chromatography*; VCH: Weinheim, 1994. (d) Iler, R. K. *The Chemistry of Silica*; John Wiley: New York, 1979.
- (4) (a) *Handbook of Fluorous Chemistry*; Gladysz, J. A., Curran, D. P., Horvath, I. T., Eds.; Wiley-VCH: Weinheim, 2004. (b) Hartley, F. R. *Supported Metal Complexes*; D. Reidel: Dordrecht, Holland, 1985, and literature cited therein. (c) Clark, J. H. *Supported Reagents in Organic Reactions*; VCH: Weinheim, 1994. (d) Special Issue on "Recoverable Catalysts and Reagents". Gladysz, J. A., Ed. *Chem. Rev.* **2002**, *102*, No. 10. (e) *Chiral Catalyst Immobilization and Recycling*; De Vos, D. E., Vankelecom, I. F. J., Jacobs, P. A., Eds.; Wiley: VCH: Weinheim, 2000.
- (5) Gladysz, J. A. *Pure Appl. Chem.* **2001**, *73*, 1319.
- (6) For some representative examples, see: (a) Gao, H.; Angelici, R. J. *Organometallics* **1999**, *18*, 989. (b) Lu, Z.; Lindner, E.; Mayer, H. A. *Chem. Rev.* **2002**, *102*, 3543. (c) Gao, H.; Angelici, R. J. *J. Am. Chem. Soc.* **1997**, *119*, 6937. (d) McMorn, P.; Hutchings, G. J. *Chem. Soc. Rev.* **2004**, *33*, 108.
- (7) (a) Merckle, C.; Haubrich, S.; Blümel, J. *J. Organomet. Chem.* **2001**, *627*, 44. (b) Merckle, C.; Blümel, J. *Adv. Synth. Catal.* **2003**, *345*, 584. (c) Merckle, C.; Blümel, J. *Top. Catal.* **2005**, in press.

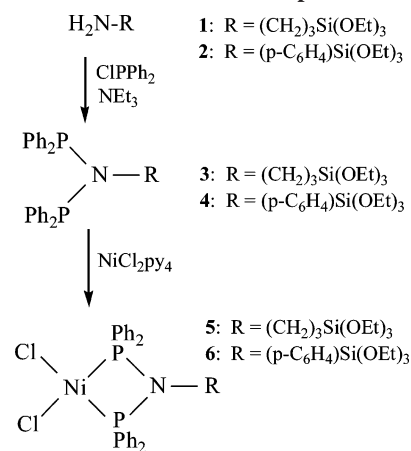
- (8) (a) Behringer, K. D.; Blümel, J. *Inorg. Chem.* **1996**, *35*, 1814. (b) Reinhard, S.; Soba, P.; Rominger, F.; Blümel, J. *Adv. Synth. Catal.* **2003**, *345*, 589.
- (9) Reinhard, S.; Behringer, K. D.; Blümel, J. *New J. Chem.* **2003**, *27*, 776.
- (10) (a) *NMR Techniques in Catalysis*; Bell, A. T., Pines, A., Eds.; Marcel Dekker: New York, 1994. (b) Engelhardt, G.; Michel, D. *High-Resolution Solid-State NMR of Silicates and Zeolites*; John Wiley & Sons: New York, 1987. (c) Fyfe, C. A. *Solid-State NMR for Chemists*; CFC Press: Guelph, Canada, 1983. (d) Stejskal, E. O.; Memory, J. D. *High-Resolution NMR in the Solid State*; Oxford University Press: New York, 1994. (e) *Solid-State NMR Spectroscopy of Inorganic Materials*; Fitzgerald, J. J., Ed.; American Chemical Society: Washington, DC, 1999. (f) Duer, M. J. *Introduction to Solid-State NMR Spectroscopy*; Blackwell Publishing: Oxford, 2004.
- (11) Reinhard, S.; Blümel, J. *Magn. Reson. Chem.* **2003**, *41*, 406.
- (12) (a) Behringer, K. D.; Blümel, J. *Z. Naturforsch.*, **B 1995**, *50b*, 1723. (b) Merckle, C.; Blümel, J. *Chem. Mater.* **2001**, *13*, 3617. (c) Posset, T.; Furrer, J.; Blümel, J. *Magn. Reson. Chem.* Manuscript in preparation.
- (13) Tsiavalariis, G.; Haubrich, S.; Merckle, C.; Blümel, J. *Synlett* **2001**, 391.
- (14) (a) Blümel, J. *J. Am. Chem. Soc.* **1995**, *117*, 2112. (b) Behringer, K. D.; Blümel, J. *J. Liq. Chromatogr.* **1996**, *19*, 2753.

metal complexes with two monodentate linkers are not necessarily bound in a chelating manner,¹⁵ again making them vulnerable to leaching.⁹ This problem can, for example, be solved by using chelating linkers.^{7–9,13} The biggest challenge, however, always arises when side products are formed on the silica surface during the immobilization process. They occupy space on the surface, depending on the reaction conditions up to 100%, while they cannot bind metal complexes. In an early study such a scenario was presented,^{16a} and recently we could determine the nature of the side products that form when ethoxysilane-modified phosphines are reacted with silica under harsh conditions with the help of ³¹P CP/MAS and model compounds: They are phosphonium salts of the type [R₃P⁺Et][SiO]⁻.^{16b} Unfortunately, in the course of our studies with a variety of linkers, metal complexes, and supports, it turned out that every new linker/support combination needs to be analyzed carefully, because different sorts of side reactions can take place, and there is no universal way to avoid any possible side product.^{16c} In this contribution, we will demonstrate one such case. We immobilized bisphosphinoamine ligands containing the ethoxysilane functionality on silica, and with the help of solid-state NMR and model reactions managed to disentangle different pathways for side reactions. Fortunately, besides the unprecedented surface chemistry, we can also present the solution for the problem, and prove that the activity of an immobilized carbonyl nickel complex depends crucially on the clean anchoring on an appropriate support.

Amines have been bound to silica via ethoxysilane groups for various applications for a long time.¹⁷ Recently, their reactions with silica have been analyzed,¹⁸ and they find new and interesting applications, for example as scavengers¹⁹ or organic catalysts.²⁰ They can be used for immobilizing dendrimers on oxidic surfaces,²¹ or after suitable modification, surface-bound amines can even be transformed into microreactors.²²

Equally popular as amines are phosphines as ligands for metal complexes, and therefore the combination of both has recently attracted much attention, for example in anchored ligands of the type R–N(CH₂PPh₂)₂.²³ The versions without methylene groups, the bisphosphinoamines R–N(PR'₂)₂, due to their interesting reactivity, have been studied since more than 20 years ago,²⁴ and this subject gets even more attention

Scheme 1. Synthesis of Bisphosphinoamine Linkers 3 and 4 and Their Dichloronickel Complexes 5 and 6



nowadays.²⁵ At present they are furthermore attractive targets because of their singular coordinating properties that are partly correlated with their large bite angles.²⁶ Recently, in their ethoxysilane-modified versions, they have also been successfully applied to immobilizing metal complexes.²⁷ Therefore, we sought to use them as linkers for our catalysts, and to study their behavior, especially with respect to their surface chemistry, in more detail with the help of solid-state NMR and model compounds.

Results and Discussion

Synthesis of Compounds. The ethoxy-modified amines **1** and **2** (Scheme 1) are commercially available. They can easily be converted into the corresponding bisphosphinoamines **3** and **4** (Scheme 1) by a reaction described by Braunstein et al.^{27b} Disregarding side reactions (see below), their immobilization should result in **3i** (Scheme 3) and **4i** (Scheme 5). Using NiCl₂py₄ as the precursor, both bisphosphinoamines bind to the metal readily and form the diamagnetic dichloronickel complexes **5** and **6**.

The dicarbonylnickel complexes **7** and **8** can be obtained via two different routes (Scheme 2). The nickel complexes **5** and **6** can be reduced by Zn in a CO stream in analogy to the procedure given in ref 8b, because the bisphosphinoamine linkers, despite the Si(OEt)₃ groups, are rather robust. This procedure is rather convenient, leading to **7** and **8** in about 82 and 80% yield. Alternatively, (COD)₂Ni can be chosen as the precursor, treated with **3**, and subsequently with CO,

(15) Behringer, K. D.; Blümel, J. *J. Chem. Soc., Chem. Commun.* **1996**, 653.

(16) (a) Blümel, J. *Inorg. Chem.* **1994**, *33*, 5050. (b) Sommer, J.; Yang, Y.; Rambow, D.; Blümel, J. *Inorg. Chem.* **2004**, *43*, 7561. (c) Posset, T.; Diploma Thesis, University of Heidelberg, 2004.

(17) (a) Tanaka, K.; Shinoda, S.; Saito, Y. *Chem. Lett.* **1979**, 179. (b) Deschler, U.; Kleinschmit, P.; Panster, P. *Angew. Chem.* **1986**, *98*, 237.

(18) Ek, S.; Iiskola, E. I.; Niinistö, L.; Pakkanen, T. T.; Root, A. *Chem. Commun.* **2003**, 2032.

(19) (a) Macquarrie, D. J.; Rousseau, H. *Synlett* **2003**, 244. (b) Westhus, M.; Gonthier, E.; Brohm, D.; Breinbauer, R. *Tetrahedron Lett.* **2004**, *45*, 3141.

(20) (a) Macquarrie, D. J.; Jackson, D. B. *Chem. Commun.* **1997**, 1781. (b) Hamaya, J.; Suzuki, T.; Hoshi, T.; Shimizu, K.-I.; Kitayama, Y.; Hagiwara, H. *Synlett* **2003**, 873.

(21) Caminade, A.-M.; Majoral, J.-P. *Acc. Chem. Res.* **2004**, *37*, 341.

(22) Wu, D.-Y.; Chen, B.; Fu, X.-G.; Wu, L.-Z.; Zhang, L.-P.; Tung, C.-H. *Org. Lett.* **2003**, *5*, 1075.

(23) Gonthier, E.; Breinbauer, R. *Synlett* **2003**, 1049. (b) Posset, T.; Blümel, J. Manuscript in preparation.

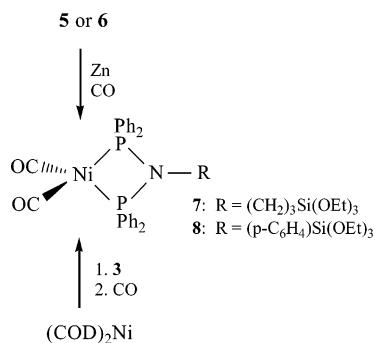
(24) (a) Schmidbaur, H.; Lauteschläger, S.; Köhler, F. H. *J. Organomet. Chem.* **1984**, *271*, 173. (b) Braunstein, P.; Hasselbring, R.; DeCian, A.; Fischer, J. *Bull. Soc. Chim. Fr.* **1995**, *132*, 691.

(25) (a) Fei, Z.; Scopelliti, R.; Dyson, P. J. *Dalton Trans.* **2003**, 2772. (b) Fei, Z.; Scopelliti, R.; Dyson, P. J. *Eur. J. Inorg. Chem.* **2004**, 530. (c) Renard, P.-Y.; Vayron, P.; Mioskowski, C. *Org. Lett.* **2003**, *5*, 1661.

(26) (a) Sushev, V. V.; Kornev, A. N.; Fedotova, Y. V.; Kursky, Y. A.; Mushtina, T. G.; Abakumov, G. A.; Zakharov, L. N.; Rheingold, A. L. *J. Organomet. Chem.* **2003**, *676*, 89. (b) Valderrama, M.; Contreras, R.; Boys, D. J. *Organomet. Chem.* **2003**, *665*, 7. (c) Balakrishna, M. S.; Reddy, V. S.; Krishnamurthy, S. S.; Nixon, J. F.; St. Laurent, J. C. T. R. B. *Coord. Chem. Rev.* **1994**, *129*, 1.

(27) (a) Chouleb, A.; Braunstein, P.; Rosé, J.; Bouaoud, S.-E.; Welter, R. *Organometallics* **2003**, *22*, 4405. (b) Braunstein, P.; Kormann, H.-P.; Meyer-Zaika, W.; Pugin, R.; Schmid, G. *Chem. Eur. J.* **2000**, *6*, 4637. (c) Bachert, I.; Braunstein, P.; Hasselbring, R. *New J. Chem.* **1996**, *20*, 993.

Scheme 2. Synthesis of Carbonylnickel Complexes 7 and 8



giving the carbonylnickel complex **7** in 71% yield. Surely, the latter route would be applicable to **8** too, but the Zn reduction is clearly more convenient and clean, and it does not require the sensitive $(\text{COD})_2\text{Ni}$ starting material.

Analytic Features of the Molecular Compounds. The NMR signal assignments of the soluble molecular compounds have all been done by standard one- and two-dimensional techniques, and for **3** they are in good agreement with those given in ref 27b. In looking at the ^{13}C NMR spectra of **3** and **4**, the most interesting features are the aryl carbon signals, all of which are triplets. Various low temperature and ^1H and ^{31}P decoupling experiments confirm that these are due to phosphorus coupling. Accordingly, we suggest that the triplets arise from “virtual coupling”, in which the signals appear equally coupled to both phosphorus nuclei.²⁸ The dichloronickel complexes **5** and **6** were not soluble in the usual organic solvents, and therefore they were characterized fully by ^{13}C , ^{31}P , and ^{29}Si CP/MAS NMR spectroscopy as polycrystalline powders. Figure 1 shows for example the ^{31}P CP/MAS spectrum of **5** at different rotational frequencies.

Interestingly, the interaction with the quadrupolar nucleus ^{14}N does not seem to broaden the lines substantially. Furthermore, it is important to note that, although both phosphorus nuclei are in such close proximity within the molecule, and definitely not “chemically dilute”, obviously their dipolar interactions can be removed efficiently already at the comparatively low spinning speed of 4 kHz. Since the spectrum could be obtained after a couple minutes, we also recorded the wide-line spectrum of **5** without rotation. The range of the chemical shift anisotropy (CSA) with the estimated values for its principal components, $\delta_{11} = 80$, $\delta_{22} = 30$, $\delta_{33} = -10$ ppm, is rather large ($\delta_{11} - \delta_{33}$ is about 90 ppm), but not unusual for a ^{31}P signal of a phosphine coordinated to a NiCl_2 moiety.¹¹ Interestingly, in contrast to earlier findings on chloronickel phosphine complexes¹¹ the residual lines, including the isotropic line, are not split in the spectrum of **5** (Figure 1). Perhaps the nature of **5** is more amorphous than crystalline due to the alkyl chain. The latter is also responsible for **3** being a liquid, while the stiff aryl ligand **4** has a melting point of 151 °C.

For complex **6** we find the usual scenario of two isotropic lines (Figure 2) at 40.0 and 47.8 ppm in the ^{31}P CP/MAS

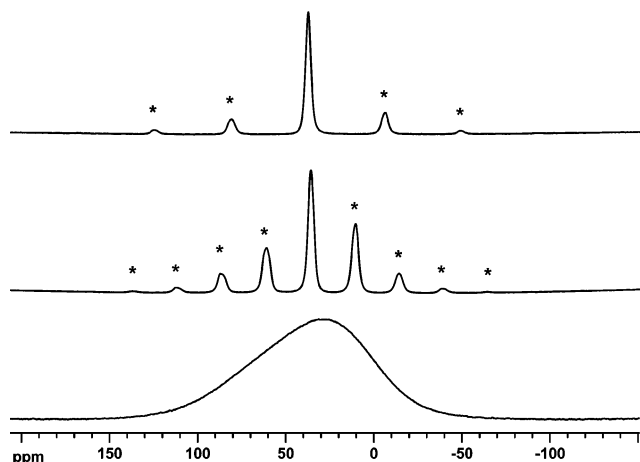


Figure 1. 161.5 MHz ^{31}P CP/MAS spectra of the polycrystalline dichloronickel complex **5** at rotational frequencies 7 (top), 4 (middle), and 0 kHz (bottom). Rotational sidebands are denoted by asterisks. For details of the measurements, see ref 11.

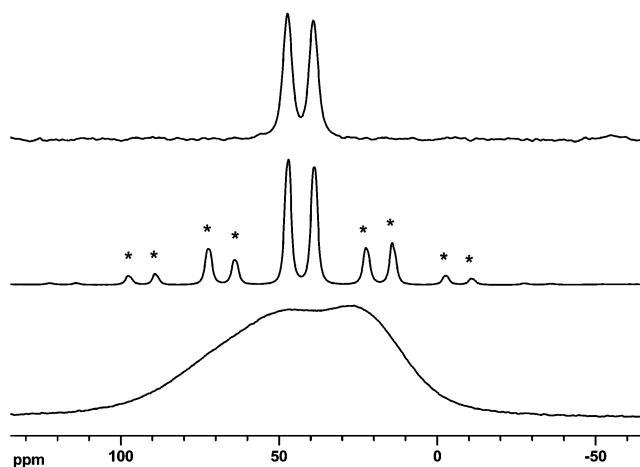


Figure 2. 161.5 MHz ^{31}P CP/MAS spectra of polycrystalline dichloronickel complex **6** at rotational frequencies 15 (top), 7 (middle), and 0 kHz (bottom). Rotational sidebands are denoted by asterisks. For details of the measurements, see ref 11.

spectrum. In accord with the spectrum of **5** and previous work,¹¹ the residual line widths of the peaks are rather small. The spectrum presented in Figure 2 is also a textbook example for the fact that both signals can have different CSAs, as the different heights and intensities of their corresponding rotational sidebands reveals. This phenomenon is also nicely visible in the wide-line spectrum (Figure 2, bottom), which has two maxima, because the center of gravity for the signal with 40.0 ppm isotropic chemical shift is more on the high-field side, while the opposite is the case for the 47.8 ppm signal. The overall range of the CSA ($\delta_{11} - \delta_{33}$) of both signals is about the same, and can roughly be estimated to be around 80 ppm.

The ^{29}Si CP/MAS spectra of **5** and **6** gave one signal for each compound, at -44.6 and -60.1 ppm, respectively, which is the usual alkyl- and aryloxyethylsilane chemical shift range.^{14b} The ^{13}C CP/MAS spectra of **5** and **6** in both cases gave a broad unresolved signal for the phenyl carbon nuclei centered around 128 ppm, as well as narrow signals for the ethoxy carbons at 20.1 and 58.7 ppm (methyl and methylene groups of **5**), and at 17.7 and 59.5 ppm (**6**). The signals of the alkyl chain of **5** could not be detected unequivocally.

(28) (a) Harris, R. K. *Can. J. Chem.* **1964**, *42*, 2275. (b) Hersh, W. H.; Xu, P.; Wang, B.; Yom, J. W.; Simpson, C. K. *Inorg. Chem.* **1996**, *35*, 5453. (c) Hersh, W. H. *J. Chem. Educ.* **1997**, *74*, 1485.

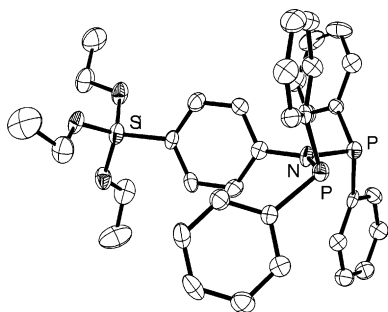


Figure 3. Molecular structure of **4**. Anisotropic replacement parameters are shown at 50% probability level; hydrogen atoms have been omitted for clarity. For details of the measurement, see ref 29. Selected angles [deg] and bond lengths [Å]: P–N–P 113.64(18); P–N–C 123.4(2)/123.0(3); P–N 1.732(3)/1.720(3); C–N 1.447(5).

Fortunately, we could also obtain single crystals of one bisphosphinoamine ligand (**4**)²⁹ and of one carbonylnickel complex (**7**).³² This is rather unusual, because normally compounds incorporating the Si(OEt)₃ group are oily or waxy materials, which refuse to crystallize. The X-ray structure of **4** is displayed in Figure 3.²⁹

It has several interesting features. First, the nitrogen atom is incorporated in trigonal planar surroundings, in accord with earlier reports on unsubstituted bisphosphinoamines.²⁵ This

(29) Colorless crystal (polyhedron); dimensions 0.10 × 0.07 × 0.04 mm³; crystal system triclinic; space group *P*1; *Z* = 2; *a* = 10.2470(6) Å; *b* = 11.0393(6) Å; *c* = 15.7646(8) Å; α = 71.4080(10)°; β = 79.9270(10)°; γ = 81.1320(10)°; *V* = 1654.89(16) Å³; ρ = 1.252 g/cm³; *T* = 200(2) K; $2\theta_{\max}$ = 23.26°; radiation Mo K α , λ = 0.710 73 Å; 0.3° ω -scans with CCD area detector, covering a whole sphere in reciprocal space; 8759 reflections measured, 4741 unique (*R*(int) = 0.0786), 2349 observed (*I* > 2 σ (*I*)); intensities corrected for Lorentz and polarization effects; empirical absorption correction applied using SADABS³⁰ based on the Laue symmetry of the reciprocal space; μ = 0.20 mm⁻¹; structure solved by direct methods and refined against *F*² with a full-matrix least-squares algorithm using the SHELXTL-PLUS (5.10) software package;³¹ 391 parameters refined; hydrogen atoms treated using appropriate riding models; goodness of fit 0.93 for observed reflections; final residual values *R*1(*F*) = 0.053, *wR*(*F*²) = 0.076 for observed reflections; residual electron density –0.27 to 0.24 e Å⁻³. Further crystallographic data for this structure have been deposited with the Cambridge Crystallographic Data Center as Supplementary Publication No. CCDC 249225. These data can be obtained free of charge via www.ccdc.cam.ac.uk/conts/retrieving.html (or from the CCDC, 12 Union Road, Cambridge CB2 1EZ, UK; fax: +44 1223 336033; e-mail: deposit@ccdc.cam.ac.uk).

(30) Sheldrick, G. M. *Program SADABS V2.03 for absorption correction*; Bruker Analytical X-ray Division: Madison, WI, 2001.

(31) Sheldrick, G. M. *Software package SHELXTL V5.10 for structure solution and refinement*; Bruker Analytical X-ray Division: Madison, WI, 1997.

(32) Yellow crystal (polyhedron); dimensions 0.30 × 0.20 × 0.10 mm³; crystal system triclinic; space group *P*1; *Z* = 2; *a* = 9.0812(2) Å; *b* = 11.7126(3) Å; *c* = 17.4888(4) Å; α = 96.35°; β = 103.6230(10)°; γ = 92.05°; *V* = 1793.08(7) Å³; ρ = 1.305 g/cm³; *T* = 200(2) K; $2\theta_{\max}$ = 27.47°; radiation Mo K α , λ = 0.710 73 Å; 0.3° ω -scans with CCD area detector, covering a whole sphere in reciprocal space; 18 528 reflections measured, 8149 unique (*R*(int) = 0.0381), 5992 observed (*I* > 2 σ (*I*)); intensities corrected for Lorentz and polarization effects; empirical absorption correction applied using SADABS³⁰ based on the Laue symmetry of the reciprocal space; μ = 0.70 mm⁻¹; *T*_{min} = 0.82, *T*_{max} = 0.93; structure solved by direct methods and refined against *F*² with a full-matrix least-squares algorithm using the SHELXTL-PLUS (5.10) software package;³¹ 406 parameters refined; hydrogen atoms treated using appropriate riding models; goodness of fit 1.11 for observed reflections; final residual values *R*1(*F*) = 0.053, *wR*(*F*²) = 0.129 for observed reflections; residual electron density –0.72 to 0.86 e Å⁻³. Further crystallographic data for this structure have been deposited with the Cambridge Crystallographic Data Center as Supplementary Publication No. CCDC 249226. These data can be obtained free of charge via www.ccdc.cam.ac.uk/conts/retrieving.html (or from the CCDC, 12 Union Road, Cambridge CB2 1EZ, UK; fax: +44 1223 336033; e-mail: deposit@ccdc.cam.ac.uk).

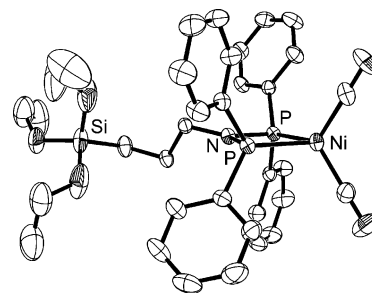


Figure 4. Crystal structure of **7**. Anisotropic replacement parameters are shown at 50% probability level; hydrogen atoms have been omitted for clarity. For details of the measurement, see ref 32. Selected angles [deg] and bond lengths [Å]: P–N–P 102.12(15); P–Ni–P 73.68(3); N–P–Ni 91.83(10)/92.28(10); P–N–C 128.4(2)/128.7(2); P–N 1.716(3)/1.704(3); C–N 1.474(4); P–Ni 2.2163(10)/2.2205(10).

shows that there must be ample electron delocalization over the P–N–P system. Preliminary theoretical studies are in accord with this geometry as the most stable arrangement.³³ Then, surprisingly, the para-substituted phenyl group is tilted in such a way that its p-orbitals are perpendicular to the one of the N atom, and this in turn is perpendicular to the P lone pair orbitals. Whether this is due to the crystal packing or whether it gives the compound a stable minimum energy constellation is not obvious at present. The angle P–N–P (113.6°) of the free ligand is larger than in its metal complexes (e.g., ref 25b) and thus nicely complements the smaller analogous angles of dppe and dppp-type ligands that we studied earlier.^{7–9} The structure of **4** with its phosphorus-bound phenyl groups bent backward already implies that it readily coordinates to metal fragments.

The crystal structure of the dicarbonylnickel complex **7** is displayed in Figure 4.³² As the NMR characteristics already implied, the structure around the Ni center is tetrahedral, while the surroundings of the nitrogen atom remain trigonal and planar. All other features of the structure are very similar to the ones of related Pd and Pt complexes, as described by Dyson and co-workers.^{25b} The P–N–P angle of 102.1° is substantially smaller now than in **4**, to accommodate the dicarbonylnickel moiety. To sustain the four-membered metallacycle, the P–Ni–P angle with 73.7° is much smaller than the ideal tetrahedral angle also. Both N–P–Ni angles correspond, with 91.8° and 92.3°, very well to the ones required for an optimal quadratic geometry. Therefore, overall, in this case the nickel center and the ligand compromise on the bite angle issue in order to form the stable complex **7**.

All the compounds **3–8** are moderately air sensitive, forming phosphine oxides after prolonged exposition to oxygen. As an example, **3** could easily be oxidized to the bisphosphine dioxide **9**.

Reactions with Oxidic Supports and Catalysis. When **7** is reacted with neutral and rigorously dried alumina, the immobilized catalyst **7i**-{Al₂O₃} is formed exclusively. The clean immobilization can be demonstrated by its ³¹P CP/MAS spectrum (Figure 5) at 4 and 10 kHz rotational frequencies. This is a typical spectrum that we are used to from earlier studies.^{8,9,16} It shows that there are no uncomplexed phosphines, and no major amounts of side products

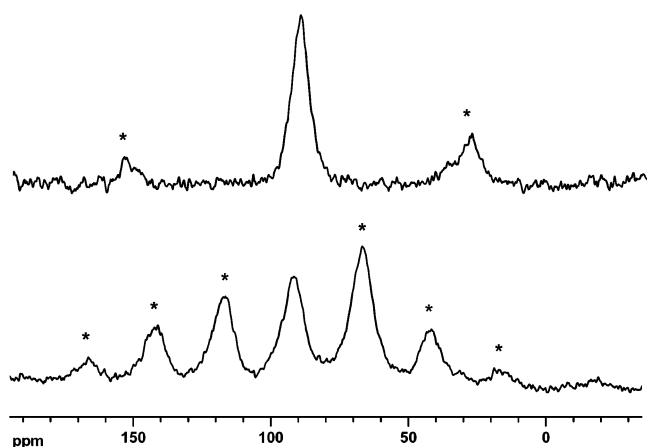


Figure 5. 161.5 MHz ^{31}P CP/MAS spectra of immobilized catalyst **7i**- $\{\text{Al}_2\text{O}_3\}$ at rotational frequencies 10 (top) and 4 kHz (bottom). The isotropic line has a chemical shift of 91.1 ppm; the ones denoted by asterisks are rotational sidebands. For details of the measurements, see ref 11.

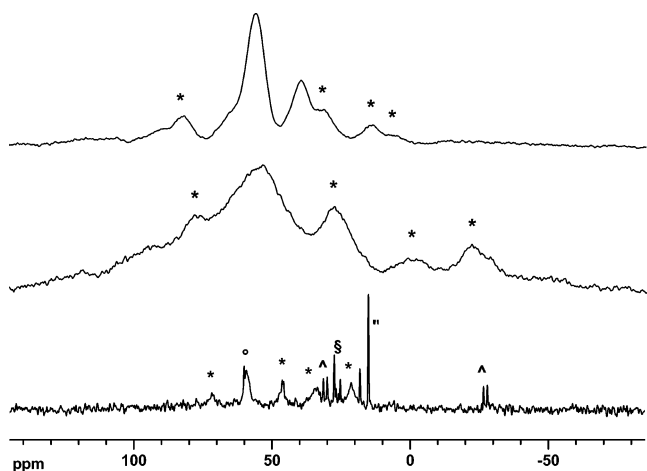


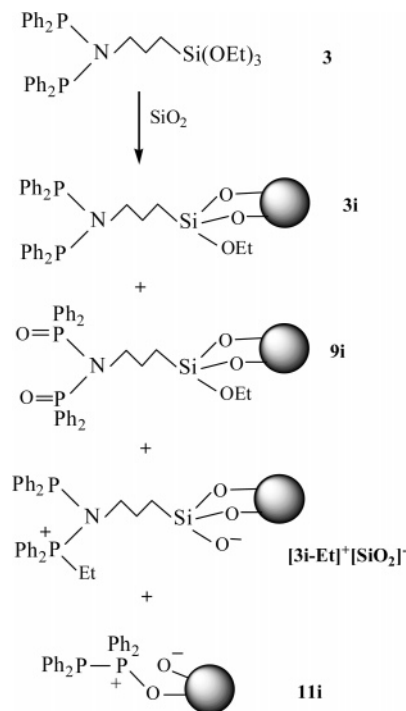
Figure 6. 161.5 MHz ^{31}P NMR spectra: CP/MAS spectrum of silica-bound linker **3i** (middle, 4 kHz), ^{31}P suspension NMR spectrum of silica-bound linker **3i** at 2 kHz (bottom), and ^{31}P CP/MAS spectrum of polycrystalline $[\mathbf{10}\text{-Et}]^+[\text{BF}_4]^-$ at 4 kHz (top). Rotational sidebands are denoted by asterisks. For details of the interpretation and signal assignment, see text; for measurement parameters, see ref 11.

formed. Again, as in the spectra of the chloronickel complexes, the CSA is large, as can be seen from the bottom trace in Figure 5.

Surprisingly, however, when we tried to attach **7** or **8** to silica instead of alumina, no matter what tricks we used,^{12b,14,16a} the solid-state NMR spectra indicated that we had produced many side products on the surface. In our experience, most often it is the fault of the couple linker/support whenever the immobilization does not work. Therefore, we investigated the reactions of the linkers **3** and **4** with silica in more detail.

When silica is treated with **3**, the classical ^{31}P CP/MAS spectrum (middle trace of Figure 6) shows broad mountains of signals, which at 4 kHz rotational frequency reveal neither the number nor the nature of the species formed. However, the ^{31}P CP/MAS spectra at low rotational speeds guarantee optimal magnetization transfer and S/N ratio.¹¹ Additionally, they have the advantage of a fingerprint-type character, displaying besides the chemical shift values also the diagnostically valuable CSA patterns. For determining the exact number and nature of the surface species, we additionally implemented the high-power proton-decoupled ^{31}P HR-MAS

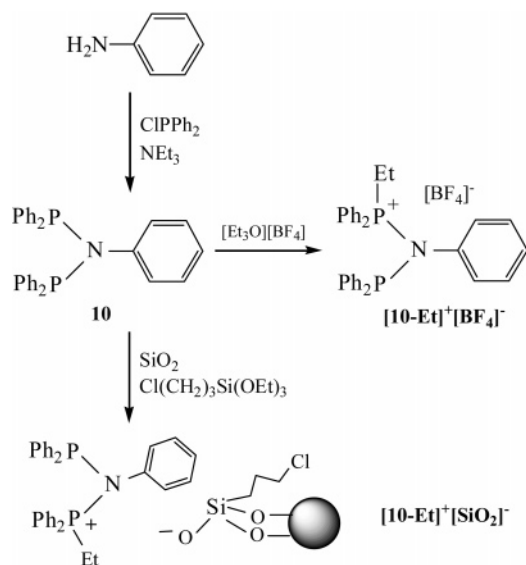
Scheme 3. Reaction of Linker **3** with Silica and Predominant Reaction Products



of a suspension of the silica in acetone, which provided us already at the low spinning speed of 2 kHz with the very well resolved spectrum displayed at the bottom of Figure 6. Herewith, one can determine the number of side products, and mostly also their nature (Scheme 3), because the CSA as well as the residual line widths are reduced substantially due to mobility in the presence of a solvent.

The suspension MAS spectrum shows that, in contrast to what one would have predicted from the CP/MAS spectrum, indeed the major part of the material consists of the desired immobilized linker **3i**- $\{\text{SiO}_2\}$ (since the rest of the manuscript will deal with silica only, for clarity we will omit $\{\text{SiO}_2\}$ in the following). Besides the isotropic line at about 60 ppm (62.0 ppm in C_6D_6 solution), denoted by a circle in the spectrum, **3i** displays a row of rotational sidebands, which are denoted by asterisks in Figure 6. The isotropic line should be in the center of gravity of the solid-state NMR signal. However, the intensity and residual half-width of the suspension NMR line at about 60 ppm imply that there must be the signal of a second species hiding underneath. We know from previous studies that one recurring immobilization side product is ethylphosphonium salt.¹⁶ Therefore, we prepared **10** and the monoethylphosphonium salt $[\mathbf{10}\text{-Et}]^+[\text{BF}_4]^-$ starting from aniline according to the procedure described above and in ref 16b (Scheme 4).

The ^{31}P CP/MAS spectrum of polycrystalline $[\mathbf{10}\text{-Et}]^+[\text{BF}_4]^-$ (Figure 6, upper trace) shows an intensive resonance at about 58 ppm, which most probably stems from the nonquaternized Ph_2P moiety of $[\mathbf{10}\text{-Et}]^+[\text{BF}_4]^-$. The $[\text{Ph}_2\text{-PEt}]^+$ moiety of $[\mathbf{10}\text{-Et}]^+[\text{BF}_4]^-$ can be attributed to the signal at about 38 ppm.^{16b} As the work by Schmutzler et al. suggests,³⁴ there should be no doubly quaternized product. Comparing the upper and lower traces in Figure 6 suggests that the overlapping signal of the latter at about 60 ppm

Scheme 4. Model Reactions with Bisphosphinoamine 10^a

^a For details, see text.

belongs to the ethylated phosphonium moiety of [3i-Et]⁺, while the Ph₂P group corresponds to the signal at 35 ppm, overlapping with a rotational sideband. The signal at 28 ppm, denoted by § in the spectrum, could stem from the doubly oxidized 9i. The signal of independently synthesized molecular 9 is found at 28.4 ppm in acetone-*d*₆ solution. As will be proven below, the two doublets at -28 and 30 ppm, denoted by ^ (Figure 6), belong to Ph₂PP(O)Ph₂, the singlet at 15 ppm, denoted by ", to surface-bound Ph₂P(O)P(O)Ph₂.

When silica is treated with **4**, the obtained material results in the ³¹P CP/MAS spectrum displayed as the bottom trace in Figure 7.

Besides the desired resonance at about 65 ppm there is clearly another signal underneath at slightly higher field, because of the irregular shape of the signal. Additionally, there is another huge signal at about -20 ppm. To test whether the overlapping signal at about 60 ppm again stems from a phosphonium-type species, we used a trick tested successfully formerly,¹⁶ and reacted the model compound **10** together with Cl(CH₂)₃Si(OEt)₃ with silica (Scheme 4). Indeed, a surface-bound version of **10** with a chemical shift of about 60 ppm for the nonethylated moiety of **10i** appeared in the ³¹P CP/MAS spectrum (top trace of Figure 7), in addition to a second signal of **10i** at about 28 ppm, which can be attributed to the [Ph₂Pt]⁺ moiety of [10-Et]⁺[SiO₂]⁻. Both signals correspond well to the resonances of the polycrystalline ethylated [10-Et]⁺[BF₄]⁻ and [3i-Et]⁺ (Figure 6, Schemes 3 and 4). Therefore, the influence of the ethoxysilane group, as in former cases,¹⁶ could also be responsible for the formation of one side product during the immobilization of **4**.

Next, we sought to clarify the nature of the second unwanted signal at -20 ppm (Figure 8, Scheme 5). For this purpose we once again recorded the suspension ³¹P HR-MAS spectrum of **4i** with its side products (Figure 8, bottom trace).

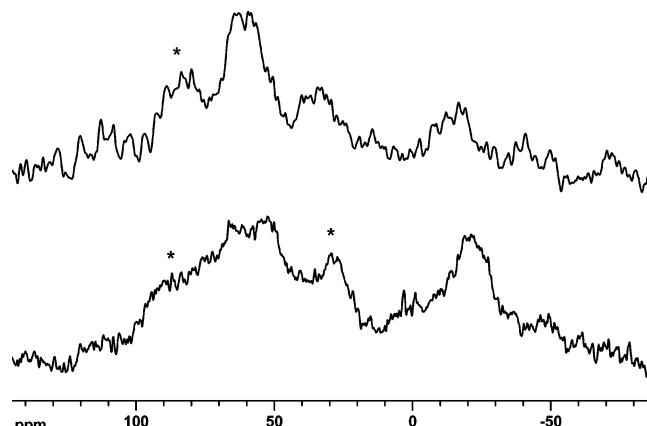


Figure 7. 161.5 MHz ³¹P CP/MAS spectra at 4 kHz rotational speed of silica-bound linker **4i** (bottom), and of silica treated with **10** and Cl(CH₂)₃Si(OEt)₃ (top). Rotational sidebands are denoted by asterisks.

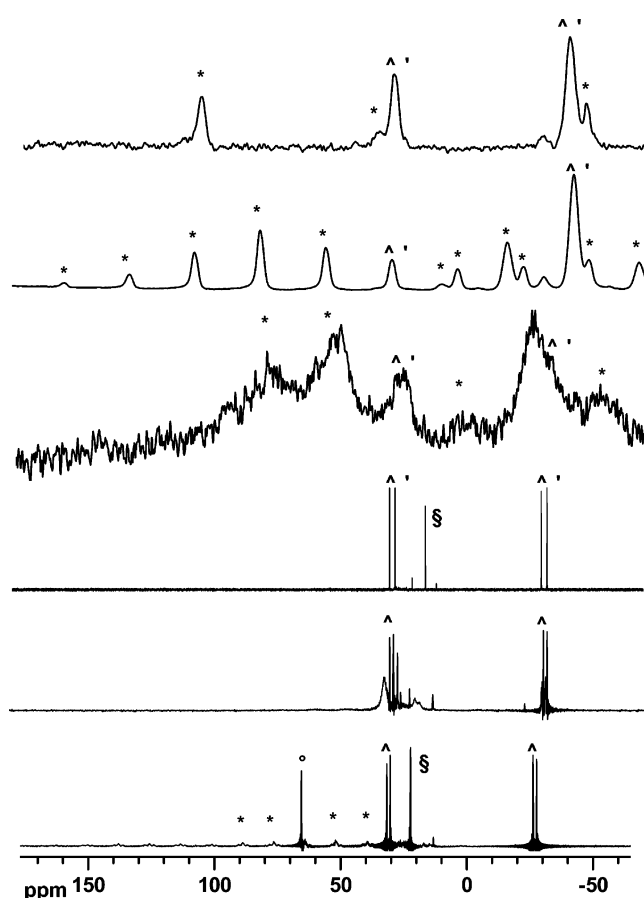
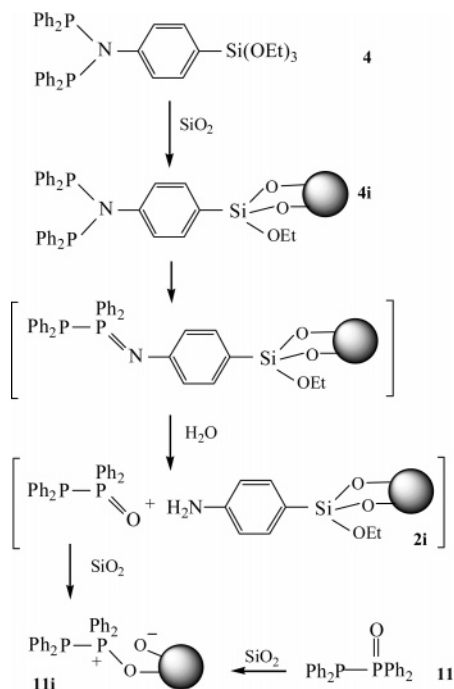


Figure 8. 161.5 MHz ³¹P NMR spectra: ³¹P suspension NMR spectrum of silica-bound linker **4i** at 2 kHz (bottom); suspension NMR spectrum of silica-bound **11i** at 2 kHz (second from bottom); solution NMR spectrum of **11** in C₆D₆ (third from bottom); ³¹P CP/MAS spectrum of silica-bound **11** (third from top, 4 kHz); ³¹P CP/MAS spectra of polycrystalline **11** at 4 and 12 kHz (second from top and top). Rotational sidebands are denoted by asterisks. For details of the spectra, see text; for measurement parameters, see ref 11.

Besides the signal of **4i** at 65 ppm there are two prominent doublets at -27 and 33 ppm with a coupling constant of 146 Hz. This corresponds very well to the data of independently synthesized Ph₂PP(O)Ph₂ (**11**) with chemical shifts of 34.0 and -23.7 ppm and ¹J(P-P) of 218.5 Hz in C₆D₆ solution (trace three from bottom in Figure 8). The signal at 18 ppm in the last spectrum belongs to the fully oxidized

(34) Karacar, A.; Klaukien, V.; Freytag, M.; Thönnessen, H.; Omelanczuk, J.; Jones, P. G.; Bartsch, R.; Schmutzler, R. Z. Anorg. Allg. Chem. 2001, 627, 2589.

Scheme 5. Reactions of **4 and **11** with Silica and Their Predominant Reaction Products**



compound $\text{Ph}_2\text{P}(\text{O})\text{P}(\text{O})\text{PPh}_2$. The latter could be responsible for the signal at 21 ppm in the spectrum of **4i** (lowest trace in Figure 8), and could stem from the oxidation of the side product **11**. We wondered why **11** would bind irreversibly to silica, and would not be removed by the usual workup of immobilization, including thorough washing of the modified silica with solvents. Therefore, we treated silica with **11** according to the usual immobilization procedure (Scheme 5), and washed the material thoroughly. Indeed, the ^{31}P HR-MAS spectrum of the material in acetone (second from bottom in Figure 8) showed, besides some yet unidentified specimens, the typical doublet of **11i**, with the reduced coupling constant as compared to **11** in solution. This effect is obviously due to the binding of **11** to the surface, which changes the “pathway” of the scalar coupling. The classical ^{31}P CP/MAS spectrum of **11i** is displayed as the third from top trace in Figure 8. Naturally, due to the lack of mobility in the absence of a solvent, the lines are broader. However, it is obvious that the Ph_2P signal can be found in its predicted position at about -28 ppm. Interestingly, in the solid the signal of the surface-bound $\text{Ph}_2\text{P}(\text{O})$ group is shifted to the higher field to about 22 ppm. This isotropic signal is much less intense than its first-order rotational sideband on the low-field side, here at 48 ppm. This point needed to be addressed. Therefore, we measured the ^{31}P CP/MAS spectra of polycrystalline **11** at different rotational frequencies.

The two upper traces in Figure 8 show spectra of **11** at 4 and 12 kHz spinning speed. Indeed, the line at about 25 ppm is the isotropic one, while the shift anisotropy pattern is far-reaching (some sidebands in the top two spectra are clipped at the rims), and many rotational sidebands, especially the low-field ones, have higher intensity than the isotropic line. Taking a closer look at the ^{31}P CP/MAS spectrum of **11i** (third from top in Figure 8) shows that there is a plethora of broad rotational sidebands spanning at least from 90 to -50

ppm that, due to their large half-widths, one could easily mistake for a rolling baseline.

Since it was not known in the literature other than with additional amines in the crystal,³⁵ we also did an X-ray analysis of a single crystal of **11**,³⁶ which was unfortunately disordered, but nevertheless proved the presence of one oxygen atom per two phosphorus moieties.^{16c} Cocrystallization of tetraphenyldiphosphine and its dioxide in a 1:1 ratio could be excluded by the NMR spectrum of the crystalline material.

It should be emphasized that all the side products identified above have never been detected in the supernatant solutions after immobilization. Only clean **3**, **4**, **7**, or **8** was present in solution, in case an excess was employed. Therefore, the side reactions are only taking place at the silica surface. Therefore, the next question to address is how **11i** can be formed from **3i** and **4i**. No traces of **11** could ever be detected in solutions of **3** and **4** or in reaction mixtures during their syntheses.

We suggest that the phosphonium species, as displayed in Schemes 3–5, are formed by the transfer of an ethyl group from one of the remaining ethoxy groups of the ethoxysilane reagent to the corresponding phosphine moiety of the bisphosphinoamines. This process has been studied and described in detail previously.¹⁶

While it has been demonstrated above that **11** binds easily and irreversibly to silica as **11i**, the next question about how the tetraphenyldiphosphine oxide **11** is formed in the first place remains. We suppose that for both **3** and **4**, and as outlined for **4** in Scheme 5, first of all the surface-bound phosphinimine is formed from **4i**. This intermediate, which we never saw in the spectra, after hydrolysis forms the surface-bound amine **2i** and **11** that in turn binds to the surface. The impact of water in this sequence would explain why **3** and **4** produce **11** on silica, which always contains traces of water,^{3d} while they can be anchored on rigorously dried, practically water-free alumina.

Studying the recent work by Dyson et al.²⁵ gives plausible explanations for our findings. First, they, as others,^{24a} have shown that there is an equilibrium between bisphosphinoamines, containing the $\text{R}_2\text{P}-\text{NR}'-\text{PR}_2$ group (**I**), and the

(35) Ferguson, G.; Myers, M.; Spalding, T. R. *Acta Crystallogr., Sect. C* **1990**, *C46*, 122.

(36) Colorless crystal (polyhedron); dimensions $0.40 \times 0.18 \times 0.12$ mm³; crystal system triclinic; space group $P\bar{1}$; $Z = 1$; $a = 8.3635(1)$ Å; $b = 9.4250(2)$ Å; $c = 9.5109(1)$ Å; $\alpha = 79.8590(10)^\circ$; $\beta = 69.5900(10)^\circ$; $\gamma = 64.4170(10)^\circ$; $V = 633.466(17)$ Å³; $\rho = 1.254$ g/cm³; $T = 200(2)$ K; $2\theta_{\text{max}} = 27.45^\circ$; radiation Mo $K\alpha$, $\lambda = 0.71073$ Å; 0.3° ω -scans with CCD area detector, covering a whole sphere in reciprocal space; 6585 reflections measured, 2875 unique ($R(\text{int}) = 0.0235$), 2456 observed ($I > 2\sigma(I)$); intensities corrected for Lorentz and polarization effects; empirical absorption correction applied using SADABS³⁰ based on the Laue symmetry of the reciprocal space; $\mu = 0.19$ mm⁻¹; $T_{\text{min}} = 0.93$, $T_{\text{max}} = 0.98$; structure solved by direct methods and refined against F^2 with a full-matrix least-squares algorithm using the SHELXTL-PLUS (5.10) software package;³¹ 179 parameters refined; hydrogen atoms treated using appropriate riding models; goodness of fit 1.07 for observed reflections; final residual values $R1(F) = 0.041$, $wR(F^2) = 0.107$ for observed reflections; residual electron density -0.24 to 0.32 e Å⁻³. Further crystallographic data for this structure have been deposited with the Cambridge Crystallographic Data Center as supplementary publication no. CCDC 249227. These data can be obtained free of charge via www.ccdc.cam.ac.uk/conts/retrieving.html (or from the CCDC, 12 Union Road, Cambridge CB2 1EZ, UK; fax: +44 1223 336033; e-mail: deposit@ccdc.cam.ac.uk).

corresponding iminobiphosphines, incorporating the R₂P–PR=NR' functionality (**II**).²⁵ The preferential formation of **II** or **I** depends on the steric and electronic properties of the rest R'. The more electron-withdrawing the group R', the more **II** is favored. In our case, clearly the *p*-ethoxysilyl-substituted phenyl ring in **4** is more electron-withdrawing than the propyl group in **3**. Therefore, immobilizing **4** on silica, we see more of the side product **11i** than in the case of **3**. Since we are working in the absence of oxygen, we suppose that no phosphine oxide results from the hydrolysis of **3** or **4** on silica. However, the reaction of pure **11** with silica is accompanied by the formation of further oxidic species (Figure 8). We tentatively attribute this to the rearrangement of **11** to Ph₂P–O–PPh₂ that, upon hydrolysis, might give diphenylphosphine oxide Ph₂P(O)H (via Ph₂POH that was never detected on the surface or in solution), which in turn can bind to the silica surface,^{16a} giving the signal at about 31 ppm (Figure 8).

While for **4** the dominant side reaction goes via the P–P bond formation on the transition from **I** to **II**, for **3** the prevalent side product is the phosphonium species. This can easily be explained with steric reasons. Linker **3** with its flexible alkyl chain can easily bend over to the ethoxysilyl group and grab an ethyl remnant, while the stiff linker **4** has to take it from an adjacent ethoxysilyl moiety of a neighboring molecule on the surface.

Although the immobilized catalysts **7i** and **8i** contained the side products described above, nevertheless we probed the influence of these scenarios on the catalytic activity in a qualitative manner. This is important, because often catalytic activity is attributed to “metal clusters” on the oxidic surface. In such a case, the destiny of the linker should not make any difference. As a test reaction for catalysis, we chose the cyclotrimerization of phenylacetylene, because it provides us with data comparable to earlier work,^{8,9} and also because there is much interest in this reaction from theoretical³⁷ and synthetic^{8,9} points of view. The standard reaction conditions for batchwise operation described earlier have been applied.^{8b} In homogeneous phase, the molecular catalyst **7** has an activity and selectivity comparable to the known nickel complexes.^{8,9} For the immobilized species, the activity correlates with the purity of the catalysts, as determined by the solid-state NMR spectra. As anticipated, the best results were obtained with the cleanly immobilized **7i**-{Al₂O₃}, and its catalytic activity compares favorably with the activities of analogous complexes with different linkers described earlier.^{8b} Therefore, we conclude that for catalysis with immobilized specimens it is an indispensable prerequisite to check their purity with a suitable analytical tool, preferentially solid-state NMR first, prior to applying them for catalysis, and potentially making wrong judgments about the quality of the linker, the support, or the catalyst.

Conclusion

In this contribution we have presented a new attractive bisphosphinoamine linker with ethoxysilane group for the

immobilization of metal complexes on oxidic supports. This one, together with a linker already known, was immobilized on oxidic supports. In the case of silica as the support, two main side reactions could be elucidated with the help of classical ³¹P solid-state NMR and with MAS of suspensions. One side product could be determined, with the help of a model compound, as the ethylated phosphonium-type version of the linker. The other side reaction incorporated the rearrangement of the P–N–P moiety of the bisphosphinoamine linker to a P=P=N functionality, which underwent hydrolysis and formed Ph₂PP(O)Ph₂ as the side product, which was subsequently bound to the silica surface. We discussed the origin of the side reactions and presented, with the use of solid-state NMR and catalytic cyclotrimerization, a viable solution to the problem, namely immobilizing the bisphosphinoamine linkers and their metal complexes on neutral alumina instead of silica as the support. This way, a catalytic performance comparable to the optimal scenarios known from earlier work can be achieved, and this linker/support system for immobilized catalysts is ready for general application.

Experimental Section

All catalytic reactions were performed under inert gas using Schlenk techniques or in a glovebox in an oxygen-free nitrogen atmosphere. The solvents were dried by boiling them with Na (cyclooctane with CaH₂), distilled, and kept under nitrogen. The NMR spectra were recorded on Bruker instruments at the indicated magnetic fields, and the chemical shifts were referenced to TMS via the solvent peaks. All the solid-state spectra presented here were recorded on a digital Bruker Avance 400 NMR spectrometer (³¹P 161.49, ¹³C 100.58, ²⁹Si 79.46 MHz) equipped with an ultrashield wide-bore magnet, and a 4 mm multinuclear double-bearing MAS probe head. The polycrystalline molecular compounds were densely packed; modified silicas were filled loosely into the ZrO₂ rotors in a glovebox. For suspension MAS measurements commercial ZrO₂ Bruker suspension rotors with inserts were used. Cross-polarization (CP) and magic angle spinning (MAS) with rotational speeds between 0 and 15 kHz were applied, as described in the text. The ³¹P CP/MAS and suspension NMR spectra were referenced with respect to 85% H₃PO₄(aq) by setting the ³¹P NMR peak of solid (NH₄)₂H₂PO₄ to +0.81 ppm. The ²⁹Si CP/MAS spectra were referenced to external (Me₃Si)₄Si; the ¹³C CP/MAS spectra were referenced to external adamantane.³⁸ The Hartmann–Hahn matches and contact times were set as described previously.¹¹ For the exponential multiplication a line-broadening factor of 20–50 Hz was applied for spectra of immobilized species; no modification of the FID was needed for the spectra of suspensions and polycrystalline compounds. All catalysts were immobilized according to the standard procedure given earlier.^{7,8} Typical surface coverages were 11–12 molecules per 100 nm². The silica and alumina were purchased from Merck with the indicated average pore sizes (Merck silica 40–100, alumina 90); their characteristics and pretreatment have been described previously.^{12b} The catalytic runs were followed by GC. The reversed-phase silica was obtained by refluxing rigorously dried Merck silica (40) with an excess of Me₃SiOEt.^{14a} Tetraphenyldiphosphine monoxide **11** was synthesized according to ref 39. Compound **10** was synthesized using the

(37) Kirchner, K.; Calhorda, M. J.; Schmid, R.; Veiros, L. F. *J. Am. Chem. Soc.* **2003**, *125*, 11721.

(38) Hayashi, S.; Hayamizu, K. *Bull. Chem. Soc. Jpn.* **1991**, *64*, 685.

(39) Abraham, K. M.; Van Wazer, J. R. *J. Organomet. Chem.* **1975**, *85*, 41.

procedure described for **3**, and the data were in accord with those given in the references.^{25a,b,40} The ethylation of compound **10** was done as described earlier.^{16b}

Synthesis of the Bisphosphinoamine 3. This compound was synthesized using the procedure given in ref 27b for the methoxy analogue of **3**. 3-Aminopropyltriethoxysilane (1.66 g, 7.49 mmol) was dissolved with triethylamine (1.52 g, 16.52 mmol) in toluene (30 mL) and cooled to $-40\text{ }^{\circ}\text{C}$. Chlorodiphenylphosphine (3.31 g, 15.00 mmol) was added dropwise while stirring vigorously. Upon warming to ambient temperature a colorless precipitate formed. After 2 h the mixture was filtrated, the solvent was removed from the filtrate, and the residue was chromatographed with toluene using reversed-phase silica. Removal of the solvent gave **3** as a clear, viscous liquid (3.40 g, 5.77 mmol, 77%). δ_{H} (acetone- d_6 , 300.14 MHz) 8.02–7.08 (20 H, m, C_6H_5); 3.63 (6 H, q, $J(\text{HH})$ 7 Hz, CH_2O), 3.28 (2 H, qui, $J(\text{PH}) = J(\text{HH})$ 9 Hz, NCH_2); 1.22 (2 H, qui, $J(\text{HH})$ 7 Hz, $\text{CH}_2\text{CH}_2\text{CH}_2$); 1.07 (9 H, t, $J(\text{HH})$ 7 Hz, CH_3); 0.19 (2 H, t, $J(\text{HH})$ 8 Hz, SiCH_2). δ_{C} (acetone- d_6 , 75.47 MHz) 140.6 (4 C, virt. t, $J(\text{PC})$ 7 Hz, C_i); 133.4 (8 C, virt. t, $J(\text{PC})$ 11 Hz, C_o); 129.5 (4 C, s, C_p); 128.9 (8 C, virt. t, $J(\text{PC})$ 3 Hz, C_m); 58.5 (3 C, s, OCH_2); 56.6 (1 C, t, $J(\text{PC})$ 10 Hz, NCH_2); 25.5 (1 C, t, $J(\text{PC})$ 3.3 Hz, NCH_2CH_2); 18.6 (3 C, s, CH_3); 8.1 (1 C, s, CH_2Si). δ_{P} (acetone- $d_6/\text{C}_6\text{D}_6$, 121.49 MHz) 63.1/62.0 (s). $\delta_{\text{N}}\{\text{C}_6\text{D}_6, \text{DMSO-}d_6, \text{reference CO}(\text{NH}_2)_2\}$ in $\text{DMSO-}d_6$, δ_{N} 77 with respect to NH_3 δ_{N} 0.0) 41.1 (s). FAB MS 590.3 (M^+). EI MS 589.2 (M^+); 385.1 ($\text{M}^+ - (\text{CH}_2)_3\text{Si}(\text{OEt})_3$); 262.0 (PPh_3^+). HR EI MS 589.2348 (M^+ , 67.1%, calcd 589.2331); 384.1154 ($\text{M}^+ - (\text{CH}_2)_3\text{Si}(\text{OEt})_3$, 100.0%, calcd 384.1071).

Synthesis of the Bisphosphinoamine 4. *p*-Triethoxysilylaniline **2** (1.00 g, 3.92 mmol) and triethylamine (0.79 g, 8.58 mmol) were treated with chlorodiphenylphosphine (0.86 g, 3.92 mmol) in the way described for **3**. Instead of chromatography, recrystallization from toluene was applied, which afforded colorless crystals of **4** (2.52 g, 47%); mp $151\text{ }^{\circ}\text{C}$ (found: C, 68.95; H, 6.33; N, 2.46; P, 9.86%); M^+ 624. $\text{C}_{36}\text{H}_{39}\text{NO}_3\text{P}_2\text{Si}$ requires C, 69.32; H, 6.30; N 2.25; P 9.93%. δ_{H} (acetone- d_6 , 300.14 MHz) 7.59–7.44 (20 H, m, C_6H_5); 7.20 (2 H, d, $J(\text{HH})$ 8 Hz, SiCCH); 6.43 (2 H, d, $J(\text{HH})$ 8 Hz, NCCH); 3.76 (6 H, q, $J(\text{HH})$ 7 Hz, OCH_2); 1.12 (9 H, t, $J(\text{HH})$ 7 Hz, CH_3). δ_{C} (acetone- d_6 , 75.47 MHz) 139.8 (1 C, t, $J(\text{PC})$ 7 Hz, NC); 137.4 (4 C, virt. t, $J(\text{PC})$ 12 Hz, PC); 136.6 (2 C, s, SiCCH); 135.4 (1 C, s, SiC); 133.8 (8 C, virt. t, $J(\text{PC})$ 12 Hz, PCCH); 129.9 (4 C, s, *p*- C_6H_5 -P); 129.2 (2 C, t, $J(\text{PC})$ 3 Hz, NCCH); 128.9 (8 C, virt. t, $J(\text{PC})$ 7 Hz, *m*- C_6H_5 -P); 59.2 (3 C, s, OCH_2); 18.5 (3 C, s, CH_3). δ_{P} (acetone- d_6 , 121.49 MHz) 68.6 (s). EI MS 623.4 (M^+); 546.4 ($\text{M}^+ - \text{C}_6\text{H}_5$); 439.4 ($\text{M}^+ - \text{P}(\text{C}_6\text{H}_5)_2$); 262.2 (PPh_3^+). X-ray analysis, see ref 29.

Synthesis of the Dichloronickel Complex 5. To a suspension of NiCl_2py_4 (0.91 g, 2.05 mmol) in 30 mL of toluene a solution of **3** (1.21 g, 2.05 mmol) in 10 mL of toluene was slowly added dropwise. The dark red compound **5** precipitated immediately. After decanting the solvent, washing the precipitate with toluene, and drying in vacuo, a dark red powder of **5** (0.69 g, 47%, unoptimized yield) resulted that was insoluble in the usual organic solvents (THF, acetone, Et_2O , toluene, pentane) but moderately soluble in DMF; mp $240\text{ }^{\circ}\text{C}$ (decomposition). CP/MAS δ_{P} (15 kHz) 38.3 (s); δ_{Si} (4 kHz) -44.6 (s). δ_{C} (6 kHz) 147.5–111.7 (m, C_6H_5); 58.7 (m, OCH_2); 20.1 (s, CH_3); FAB MS 682.0 ($\text{M}^+ - \text{Cl}$); 588.1 ($\text{M}^+ - 2\text{Cl}$). HR FAB MS 682.1321 (100.0%, $\text{M}^+ - \text{Cl}$, calcd for $(\text{C}_{33}\text{H}_{41}\text{Cl}_2\text{NNiO}_3\text{P}_2\text{Si} - \text{Cl})$ 682.1372).

Synthesis of the Dichloronickel Complex 6. Compound **6** was synthesized from NiCl_2py_4 (0.16 g, 0.36 mmol) and **4** (0.23 g, 0.36 mmol) as described above for **5**. The orange powder (0.15 g, 55%

unoptimized yield) showed the same solubility in solvents as **5**. CP/MAS NMR δ_{P} (15 kHz) 40.0 (s)/47.8 (s). δ_{C} (6 kHz) 192.7–92.0 (m, C_6H_5); 59.5 (s, OCH_2); 17.7 (s, CH_3). δ_{Si} (4 kHz) -60.1 (s). FAB MS 716.1 ($\text{M}^+ - \text{Cl}$); 681.1 ($\text{M}^+ - 2\text{Cl}$). HR FAB MS 716.1201 (100.0%, $\text{M}^+ - \text{Cl}$, calcd for $(\text{C}_{36}\text{H}_{39}\text{Cl}_2\text{NNiO}_3\text{P}_2\text{Si} - \text{Cl})$ 716.1216).

Synthesis of the Dicarboxynickel Complex 7. *Route 1.* A solution of $(\text{COD})_2\text{Ni}$ (0.22 g, 0.79 mmol) in 20 mL of toluene was cooled to $-30\text{ }^{\circ}\text{C}$, and subsequently a solution of **3** (0.45 g, 0.79 mmol) in 10 mL of toluene was added dropwise. The color of the yellow solution turned dark red. After 30 min at $-30\text{ }^{\circ}\text{C}$, CO was bubbled through the reaction mixture for 2 h. Then the mixture was warmed to ambient temperature in a steady stream of CO. The color of the mixture became lighter again. After removal of the solvent in vacuo, **7** remained as a dark orange oil that was purified by reversed-phase chromatography (0.40 g, 71%).

Route 2. Complex **5** (0.41 g, 0.57 mmol) was dissolved in 20 mL of DMF and treated with Zn powder (0.06 g, 0.84 mmol). This mixture was stirred in a stream of CO for 1 h, during which time the color changed from red to light green. After removal of the solvent from the supernatant solution, the greenish yellow residue was dissolved in toluene and purified by reversed-phase chromatography. Complex **7** was obtained as a yellow powder (0.33 g, 82%), $\nu_{\text{max}}/\text{cm}^{-1}$ (CO) 2000s, 1935s (KBr). δ_{H} (C_6D_6 , 300.21 MHz) 7.08–7.82 (20 H, m, C_6H_5); 3.63 (6 H, q, $J(\text{HH})$ 7 Hz, OCH_2); 2.97 (2 H, qui, $J(\text{PH}) = J(\text{HH})$ 9 Hz, NCH_2); 1.38 (2 H, qui, $J(\text{HH})$ 7 Hz, NCH_2CH_2); 1.08 (9 H, t, $J(\text{HH})$ 7 Hz, CH_3); 0.15 (2 H, t, $J(\text{HH})$ 8 Hz, SiCH_2). δ_{C} (acetone- d_6 , 75.47 MHz) 200.9 (2 C, t, $J(\text{PC})$ 2 Hz, CO); 137.6 (4 C, virt. t, $J(\text{PC})$ 16 Hz, C_i); 132.9 (8 C, virt. t, $J(\text{PC})$ 8 Hz, C_o); 131.3 (4 C, s, C_p); 129.4 (8 C, virt. t, $J(\text{PC})$ 5 Hz, C_m); 58.6 (3 C, s, OCH_2); 52.2 (1 C, t, $J(\text{PC})$ 6 Hz, NCH_2); 24.6 (1 C, s, NCH_2CH_2); 18.3 (3 C, s, CH_3); 8.1 (1 C, s, SiCH_2). δ_{P} (acetone- $d_6/\text{C}_6\text{D}_6$, 121.49 MHz) 91.0/91.4. FAB MS 677.1 ($\text{M}^+ - \text{CO}$); 647.1 ($\text{M}^+ - 2\text{CO}$). UV/vis (nm) λ 260 ($\epsilon = 14\ 382$), λ 334 ($\epsilon = 7131$), λ 388 ($\epsilon = 4908$). X-ray analysis, see ref 32.

Synthesis of the Dicarboxynickel Complex 8. The chloronickel complex **6** (0.23 g, 0.36 mmol) was treated with Zn powder (0.02 g, 0.36 mmol) in the same way as described for **7**, route 2. The dicarboxynickel complex was obtained as a yellow powder (0.21 g, 80%); $\nu_{\text{max}}/\text{cm}^{-1}$ (CO) 2006s, 1943s (KBr). δ_{H} (acetone- d_6 , 300.14 MHz) 7.42–7.31 (20 H, m, *p*- C_6H_5); 7.25 (2 H, d, $J(\text{HH})$ 8 Hz, SiCCH); 6.76 (2 H, d, $J(\text{HH})$ 8 Hz, NCCH); 3.77 (6 H, q, $J(\text{HH})$ 7 Hz, OCH_2); 1.15 (9 H, t, $J(\text{HH})$ 7 Hz, CH_3). δ_{C} (acetone- d_6 , 75.47 MHz) 203.3 (2 C, t, $J(\text{PC})$ 2 Hz, CO); 139.9 (1 C, t, $J(\text{PC})$ 7 Hz, NC); 136.8 (4 C, virt. t, $J(\text{PC})$ 14 Hz, PC); 135.6 (1 C, s, SiC); 132.6 (8 C, virt. t, $J(\text{PC})$ 9 Hz, *o*- C_6H_5 -P); 131.1 (4 C, s, *p*- C_6H_5 -P); 129.0 (8 C, virt. t, $J(\text{PC})$ 5 Hz, *m*- C_6H_5 -P); 127.0 (2 C, t, $J(\text{PC})$ 2 Hz, NCCH); 58.7 (3 C, s, OCH_2); 18.5 (3 C, s, CH_3). δ_{P} (acetone- d_6 , 121.49 MHz) 96.0 (s). FAB MS 682.2 ($\text{M}^+ - 2\text{CO}$). UV/vis (nm) λ 266 ($\epsilon = 12\ 005$), 324 ($\epsilon = 4802$).

Synthesis of the Aminobisphosphinoxide 9. A solution of **3** in toluene was treated with an excess of H_2O_2 (30% in H_2O) and stirred for 30 min at ambient temperature. The organic phase was removed and dried with Na_2SO_4 . After filtration and removal of the solvent in vacuo, a colorless crystalline solid was obtained in quantitative yield; $\nu_{\text{max}}/\text{cm}^{-1}$ (PO) 1213s. δ_{H} (acetone- d_6 , 300.13 MHz) 7.85–7.36 (20 H, m, C_6H_5); 3.59 (6 H, q, $J(\text{HH})$ 7 Hz, OCH_2); 3.29 (2 H, qui, $J(\text{PH}) = J(\text{HH})$ 9 Hz, NCH_2); 1.37 (2 H, qui, $J(\text{HH})$ 7 Hz, $\text{CH}_2\text{CH}_2\text{CH}_2$); 1.06 (9 H, t, $J(\text{HH})$ 7 Hz, CH_3); 0.12 (2 H, t, $J(\text{HH})$ 8 Hz, SiCH_2). δ_{C} (acetone- d_6 , 75.47 MHz) 134.6 (4 C, virt. t, $J(\text{PC})$ 19 Hz, C_i); 133.3 (8 C, virt. t, $J(\text{PC})$ 8 Hz, C_o); 132.6 (4 C, s, C_p); 128.8 (8 C, virt. t, $J(\text{PC})$ 7 Hz, C_m); 58.6 (3 C, s, OCH_2); 50.3 (1

C, s, NC); 25.4 (1 C, s, CH₂CH₂CH₂); 18.6 (3 C, s, CH₃); 8.3 (1 C, s, SiCH₂). $\delta_p(\text{acetone-}d_6/\text{C}_6\text{D}_6, 121.49 \text{ MHz})$ 28.4/29.6. FAB MS 622.3 (M⁺, calcd for C₃₃H₄₁NO₅P₂Si 621.715). EI MS 621.0 (M⁺); 576.4 (M⁺ - OEt); 534.2 (M⁺ - (OEt)₂); 430.1 (M⁺ - (CH₂)₂Si(OEt)₃); 420.1 (M⁺ - POPh₂); 342.0 (M⁺ - POPh₃), 201.1 (POPh₂⁺). HR EI MS 621.2226 (23.90%, M⁺, calcd 621.2229); 576.1881 (17.02%, M⁺ - OEt, calcd 576.1889); 430.1120 (85.52%, M⁺ - (CH₂)₂Si(OEt)₃, calcd 430.1126); 420.1716 (50.28%, M⁺

- POPh₂, calcd 420.1760); 342.0809 (50.07%, M⁺ - POPh₃, calcd 342.1290); 201.0470 (53.78%, POPh₂⁺, calcd 201.0469).

Acknowledgment. We thank the Deutsche Forschungsgemeinschaft (DFG) for financial support via the Sonderforschungsbereich (SFB 623), and INSTRUCTION for generous cooperation (T.P.). We also thank Dr. J. Furrer for valuable advice.

CM048236F